THE JOURNAL OF PHYSICAL CHEMISTRY C LETTERS

2008, *112,* 12602–12605
Published on Web 07/31/2008

Raman Mapping Investigation of Graphene on Transparent Flexible Substrate: The Strain Effect

Ting Yu,* Zhenhua Ni, Chaoling Du, Yumeng You, Yingying Wang, and Zexiang Shen

Division of Physics and Applied Physics, School of Physical and Mathematical Sciences, Nanyang Technological University, Singapore 637371, Singapore

Received: July 9, 2008; Revised Manuscript Received: July 18, 2008

We report a Raman mapping investigation of strain effects on graphene on transparent and flexible substrate. Raman mappings reveal a significant red-shift of the 2D mode with introduction of tensile strain, distribution of local strain in the strained graphene, and immediate recovery after strain relaxation. The systematic fitting and statistical analysis quantify the tensile strain sensitivity of graphene, which is comparable to the single-walled carbon nanotubes (SWNTs) and implies the potential of graphene as an ultrasensitive strain sensor. The uniaxial strain will break the sublattice symmetry of graphene, hence changing its electronic band structures, for example, bandgap opening. This suggests the potential to desirably tune electronic band structures of graphene by controllably introducing strain.

Introduction

Graphene, a new candidate of carbon family that consists of only one plain layer of atoms arranged in a honeycomb lattice, has attracted intensive interest since it was discovered.[1] Due to its special properties like the unusual energy dispersion relation, the low-lying electrons in single-layer graphene behave like massless relativistic Dirac fermions, graphene exhibits many unique properties such as quantum spin Hall effect,[2] phase coherent transport,[3] suppression of the weak localization,[4] and deviation from the adiabatic Born−Oppenheimer approximation.[5] These properties make graphene an ideal sample for both fundamental studies and practical applications.

Graphene can be obtained by mainly two approaches: mechanical exfoliation of graphite[1] or thermal graphitization of a silicon carbide (SiC) surface.[6,7] The most common substrate used in the former method is Si with 300 nm thick SiO_2, as it offers very good optical contrast between the graphene and the surrounding[1,8] and also is a suitable substrate for device fabrication.[9] To date, very few works[9] report graphene on transparent and flexible substrates, while its counterpart, carbon nanotubes (CNTs), has been successfully deposited and even grown on several kinds of such substrates.[10] The success of building up devices on plastic significantly enriches the applications of CNTs for nanoelectric applications. Meanwhile, the plastic substrate with excellent flexibility could function as a unique platform to reveal more properties of CNTs. For example, the behavior of single-walled carbon nanotubes (SWNTs) under uniaxial strain has been systematically studied by resonance Raman scattering.[11] The results clearly demonstrate the ability of SWNTs as an ultrasensitive strain sensor. In this Letter, we report a resonance Raman mapping investigation of graphene on transparent flexible substrate. The tensile strain sensitivity of the 2D band of graphene has been obtained for the first time, and it is found to be comparable to that of SWNTs, indicating its potential as an ultrasensitive strain sensor. Moreover, the uniaxial strain on graphene may change its electronic band structures, for example, bandgap opening, which suggests the potential to desirably tune electronic band structures of graphene by controllably introducing strain. This could be very helpful and important for developing graphene based electronics. Nonuniform local strain distribution is also revealed by Raman mapping. This calls for extreme caution when we develop graphene devices, especially strained graphene, as the local electronic structure might differ from one region to the other.

Experimental Methods

The graphene sample was obtained from highly ordered pyrolytic graphite (HOPG, Structure Probe, Inc./SPI Supplies) by mechanical cleavage on polyethylene terephthalate (PET) film of thickness 0.11 mm. Tensile strain was introduced to graphene sheets on the top surface of PET film by bending the PET film. As shown in Figure 1a, the amount of strain is determined by dividing the increase in length of the strained top surface (highlighted by the red dashed line) by the unstrained length (blue dashed line). Here, we assume the thickness of PET film remains unchanged and no strain presents at the middle level (blue dashed line) of film during the bending process. The Raman spectra were carried out with a WITEC CRM200 Raman system. The excitation source is 532 nm laser (2.33 eV) with a laser power below 0.1 mW on the sample to avoid laser induced heating. A 100× objective lens with NA = 0.95 was used in the Raman experiments, and the spot size of the 532 nm laser was estimated to be 500 nm. To obtain the Raman images, a piezo stage was used to move the sample with a step size of 300 nm and a Raman spectrum was recorded at every point. The spectra were analyzed, and Raman images were then

* To whom correspondence should be addressed. E-mail: yuting@ntu.edu.sg.

10.1021/jp806045u CCC: $40.75

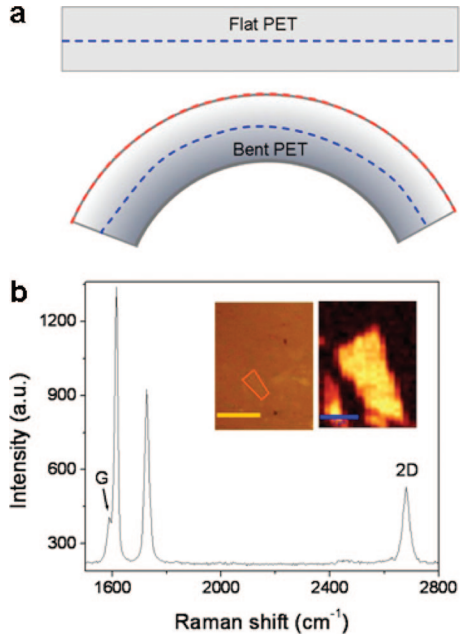

Figure 1. (a) Schematic diagram showing the flat and bent PET substrates. (b) Raman spectrum of graphene on PET. The insets show an optical image (left) and integrated Raman intensity image (right) of the 2D band. The scale bars are 10 μm (optical) and 2 μm (Raman) respectively.

constructed using a parameter (peak frequency, peak intensity, integrated peak intensity, or peak width) by using WITec Project software.

Results and Discussion

Figure 1b shows the Raman spectrum of graphene on PET. The Raman fingerprint 2D mode of the single-layered graphene sample, a sharp (~30 cm^{-1}) and symmetric peak at around 2680 cm^{-1}, clearly presents. Unfortunately, the G mode of graphene overlaps with a strong peak from PET and appears as a weak shoulder. In this work, we focus on the 2D mode of graphene, which has been detailed by Ferrari as the result of a double resonance (DR) process and the special electronic band structure of graphene.[12] The insets are the optical (left) and Raman integrated intensity image (right) of a single-layered graphene sample. The optical contrast between graphene and PET is very poor as compared to that of Si/SiO_2 substrate. By extracting the integrated intensity of the 2D mode, the Raman image of the graphene is obtained and clearly shows the dimension of the graphene. Careful examination of the Raman spectra confirms that the entire piece is made of single-layered graphene.[8]

Figure 2a presents the Raman images of unstrained (a1), strained (a2−a5), and relaxed (a6) graphene by extracting the frequency of the 2D mode. By bending the PET, a strain of 0.21% (a2), 0.36% (a3), 0.47% (a4), and 0.56% (a5) was achieved. The range of contrast scale of ALL Raman images has been fixed within the same range of 2670 (dark)−2705 cm^{-1} (bright). As reported previously,[13] even within the same piece of graphene, the frequency of the 2D mode could differ from one region to the other. This variation is clearly indicated by the frequency distribution in the Raman image (a1). Comparing the distribution of the 2D mode frequency (a1) to the peak width of this mode (Figure 3a1), the low correlation between these two parameters indicates that the nonuniformity of the 2D mode frequency of the unstrained graphene is mainly due to unintentional local doping.[14] With an increase in tensile strain

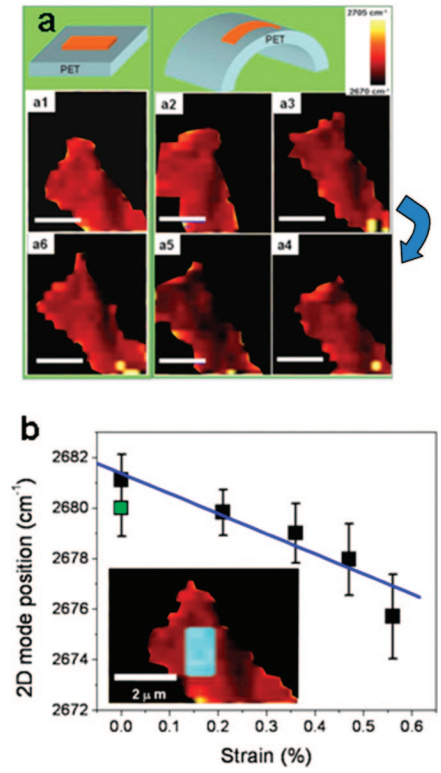

Figure 2. Raman images of (a1) unstrained graphene, (a2−a5) strained graphene, (a6) relaxed graphene by extracting 2D mode frequency. The bending/strain is in the horizontal direction. (b) Mean of the 2D mode frequency from the entire graphene as a function of strain. The error bars are the standard deviations. The data point in green is from the relaxed graphene. The inset shows the interested area subjected to the statistical analysis. Scale bar = 2 μm.

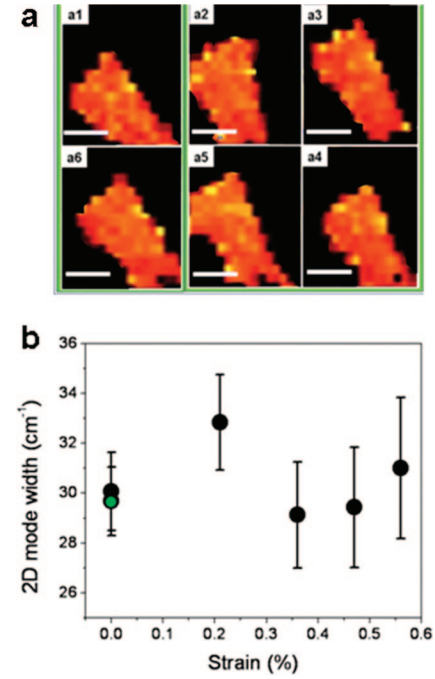

Figure 3. Raman images of (a1) unstrained graphene, (a2−a5) strained graphene, (a6) relaxed graphene by extracting 2D mode width. (b) Mean of the 2D mode line width from the graphene as a function of strain. The error bars are the standard deviations. The data point in green is from the relaxed graphene. Scale bar = 2 μm.

(a2−a5), the Raman peak of the 2D mode shows a universal red-shift over the entire strained graphene, as reflected by the

increment of darkness. With careful observation of the contrast in the Raman image of the most strained graphene here (a5), we noticed that the strain distribution is not perfectly uniform. The nonuniformity might be due to the contact, and consequently, the van der Waals force between the graphene and PET differs from region to region. Such ununiformity calls for caution on developing graphene electronics on substrates, especially when strain exists. More interesting and importantly, when the strain is released, the Raman image (a6) reverses back and shows a similar image as the original one (a1). Experimentally, we also noticed the graphene is able to recover immediately once the strain is released, while the CNTs need to take over 1 week because of slippage.[15] Such reversible and quick recovery property demonstrates the excellent elasticity of graphene, which might be critical for the practical applications.

To further quantify the tensile strain of graphene and the nonuniformity, the Raman spectra of the 2D mode from the same region of unstrained, strained, and relaxed graphene were fitted. To provide information on the pure strain effect, the region without doping is used for analysis, as highlighted in the inset of Figure 2b. The mean frequencies of the 2D mode were plotted as a function of strain, and the standard deviation was employed as errors (Figure 2b). A linear dependence of the 2D mode frequency on the strain is presented. The tensile strain causes a significant downshift of the 2D mode. The slope of the linear fitting line indicates the tensile strain sensitivity of graphene. It is -7.8 cm^{-1}/%, much bigger than that of C_{60} (-0.13 cm^{-1}/%) or multiwalled carbon nanotubes (MWNTs) (-0.48 cm^{-1}/%) and comparable to that of SWNTs (-7.9 cm^{-1}/%).[16] We have totally tested five samples. All of the samples show strain induced red-shift of the 2D band, and the strain coefficient differs from 5 cm^{-1} to 15 cm^{-1}/%. The high strain sensitivity of graphene successfully demonstrates its potential as an ultrasensitive strain sensor that is better than offered by MWCNTs.[11] Once the strain is released, the 2D shifts upward and almost back to the original position, indicating the well strain reversibility of graphene. The small frequency difference ($\sim$1 cm^{-1}) between the unstrained and relaxed sample might be because the PET substrate is not fully relaxed to the original position, and hence there is a small strain residue on the relaxed graphene. The Raman images constructed using the 2D mode peak width (full width at half-maximum) is shown in Figure 3a. Different from the 2D frequency, there is no obvious bandwidth distribution over the entire unstrained graphene. Moreover, the tensile strain shows no significant effects on the 2D mode width. The fitting and statistical analysis (Figure 3b) also confirm the weak dependence of 2D width on the strain.

The theoretical ab initio and tight binding calculations have predicted large changes in the electronic band structure of SWNTs upon application of strain,[17−19] due to the change of the circumferential quantization vector. However, there is no quantization vector in a graphene sheet. Most recently, the band structure of graphene has been successfully engineered by two probes: introducing graphene−substrate interaction and graphene−dopant coupling.[20] Similarly, in this work, we propose that the unaxial strain might distort the sublattice and eventually break the A−B symmetry of graphene, which could effectively change the electronic band structure of graphene, for example, opening a bandgap. Therefore, the strained graphene may provide an alternative way to controllably tune the band structure of graphene. In the previous work, we also observed strain in epitaxial graphene[7] as well as graphene after deposition of a SiO_2 layer and annealing.[21] The strain in those cases is biaxial, which

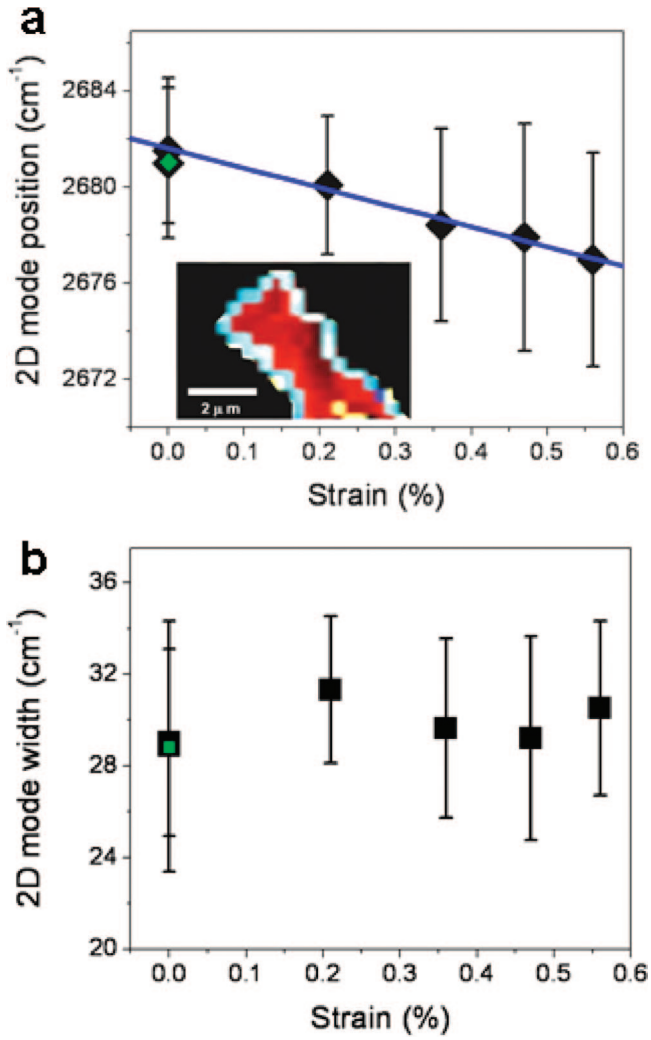

Figure 4. (a) Mean of the 2D mode frequency from the edge of graphene as a function of strain. The error bars are the standard deviation. The inset shows the interested area subjected to the statistical analysis. The scale bar is 2 μm. (b) The mean of the 2D mode line width from the corresponding edges as a function of strain. The data points in green are from the relaxed graphene.

is the difference from the uniaxial strain in the current work. Garcia-Sanchez et al. also observed the existence of nonuniform strain on graphene prepared by micromechanical cleavage.[22]

A good understanding of the edge of graphene is critical in both the fundamental study and practical applications.[23] For example, the two possible (perfect) terminations in graphene, *zigzag* and *armchair*, may substantially alter the energy properties of graphene, as zigzag edges support localized states while armchair edges do not. To reveal the strain effects on the edge of graphene, the Raman spectrum of the 2D mode from the edge of graphene was fitted and statistically analyzed. As shown in Figure 4a and b, the tensile strain results in a downshift of 2D frequency while the width does not change too much. The relatively bigger error bars here could be due to the unintentional involvement of the background information into the statistical data sample during the data selection process. Unexpectedly, the edge does not show any special strain effects, although the bonding there should be significantly different to that at the main body of graphene. This might be because the edge is confined in only a few nanometers, which contributes little to the total signal we obtained (the laser spot size is $\sim$500 nm). Further

Raman studies with higher resolution, such as near field Raman spectroscopy, will be carried out on the edge study.

Conclusion

In summary, single-layered graphene samples have been successfully deposited on transparent flexible substrate. The elastic polymer substrate allows the strain to be varied in a controllable and reversible fashion and facilities the systematical study of the strain effects on graphene. Raman mapping of the unstrained, strained, and relaxed graphene reveals that graphene is very sensitive to the tensile strain and has very good strain reversibility. Our results also directly show the nonperfect uniformity of strain distribution on graphene. The tensile strain sensitivity (-7.8 cm^{-1}/%) of graphene is further quantitatively obtained by fitting the data resulting from the graphene without unintentional doping, which is comparable to that of SWNTs and implies the potential of graphene as an ultrasensitive strain sensor, and even being better than a CNT sensor considering the instant recovery of graphene. Finally, we propose that uniaxial strain on graphene may change the band structure of graphene, such as introducing a bandgap opening, which is essential to its device application.

References and Notes

(1) Novoselov, K. S.; Geim, A. K.; Morozov, S. V.; Jiang, D.; Zhang, Y.; Dubonos, S. V.; Grigorieva, I. V.; Firsoy, A. A. *Science* **2004**, *306*, 666.

(2) Zhang, Y. B.; Tan, Y. W.; Stomer, H. L.; Kim, P. *Nature* **2005**, *438*, 201.

(3) Miao, F.; Wijeratne, S.; Zhang, Y.; Coskun, U. C.; Bao, W.; Lau, C. N. *Science* **2007**, *317*, 1530.

(4) Morozov, S. V.; Novoselov, K. S.; Kastsnelson, M. I.; Schedin, F.; Ponomarenko, L. A.; Jiang, D.; Geim, A. K. *Phys. Rev. Lett.* **2006**, *97*, 016801.

(5) Pisana, S.; Lazzeri, M.; Casiraghi, C.; Novoselov, K. S.; Geim, A. K.; Ferrari, A. C.; Mauri, F. *Nat. Mater.* **2007**, *6*, 198.

(6) Berger, C.; Song, Z. M.; Li, X. B.; Wu, X. S.; Brown, N.; Naud, C.; Mayo, D.; Li, T. B.; Hass, J.; Marchenkov, A. N.; Conrad, E. H.; First, P. N.; de Heer, W. A. *Science* **2006**, *312*, 1191.

(7) Ni, Z. H.; Chen, W.; Fan, X. F.; Kuo, J. L.; Yu, T.; Wee, A. T. S.; Shen, Z. X. *Phys. Rev. B* **2008**, *77*, 115416.

(8) Ni, Z. H.; Wang, H. M.; Kasim, J.; Fan, H. M.; Yu, T.; Wu, Y. H.; Feng, Y. P.; Shen, Z. X. *Nano Lett.* **2007**, *7*, 2758.

(9) Chen, J. J.; Ishigami, M.; Jang, C.; Hines, D. R.; Fuhrer, M. S.; Williams, E. D. *Adv. Mater.* **2007**, *19*, 3623.

(10) Hofmann, S.; Ducati, C.; Kleinsorge, B.; Robertson, J. *Appl. Phys. Lett.* **2003**, *83*, 4661.

(11) Frogley, M. D.; Zhao, Q.; Wagner, H. D. *Phys. Rev. B* **2002**, *65*, 113413.

(12) Ferrari, A. C.; Meyer, J. C.; Scardaci, V.; Casiraghi, C.; Lazzeri, M.; Mauri, F.; Piscanec, S.; Jiang, D.; Novoselov, K. S.; Roth, S.; Geim, A. K. *Phys. Rev. Lett.* **2006**, *97*, 187401.

(13) Casiraghi, C.; Pisana, S.; Novoselov, K. S.; Geim, A. K.; Ferrari, A. C. *Appl. Phys. Lett.* **2007**, *91*, 233108.

(14) Stampfer, C.; Molitor, F.; Graf, D.; Ensslin, K.; Jungen, A.; Hierold, C.; Wirtz, L. *Appl. Phys. Lett.* **2007**, *91*, 241907.

(15) Cronin, S. B.; Swan, A. K.; Ünlü, M. S.; Goldberg, B. B.; Dresselhaus, M. S.; Tinkham, M. *Phys. Rev. Lett.* **2004**, *93*, 1674011.

(16) Cooper, C. A.; Young, R. J. *J. Raman Spectrosc.* **1999**, *30*, 929.

(17) Minot, E. D.; Yaish, Y.; Sazonova, V.; Park, J. P.; Brink, M.; McEuen, P. L. *Phys. Rev. Lett.* **2002**, *90*, 156401.

(18) Heyd, R.; Charlier, A.; McRae, E. *Phys. Rev. B* **2007**, *55*, 6820.

(19) Yang, L.; Anantram, M. P.; Han, J.; Lu, J. P. *Phys. Rev. B* **1999**, *60*, 13874.

(20) Zhou, S. Y.; Gweon, G. H.; Fedorov, A. V.; First, P. N.; De heer, W. A.; Lee, D. H.; Guine, F.; Castro Neto, A. H.; Lanzara, A. *Nat. Mater.* **2007**, *6*, 770.

(21) Ni, Z. H.; Wang, H. M.; Ma, Y.; Kasim, J.; Wu, Y. H.; Shen, Z. X. *ACS Nano* **2008**, *2*, 1033.

(22) Garcla-Sanchez, D.; van der Zande, A. M.; San Paulo, A.; Lassagne, B.; McEuen, P. L.; Bachtold, A. *Nano Lett.* **2008**, *8*, 1399.

(23) Castro, E. V.; Peres, N. M. R.; Lopes dos Santos, J. M. B.; Castro Neto, A. H.; Guinea, F. *Phys. Rev. Lett.* **2008**, *100*, 026802.

JP806045U